

Orientalional Correlations Near Interfaces. Computer Simulations of Water and Electrolyte Solutions in Confined Environments

Axel Kohlmeyer, Christoph Hartnig and Eckhard Spohr ¹

*Abteilung für Theoretische Chemie, Universität Ulm,
Albert-Einstein-Allee 11, D-89069 Ulm, Germany*

We review published work and summarize the current understanding of orientational correlations in liquid water and aqueous solutions near interfaces, as obtained from computer simulation studies. We present a number of examples in which we discuss the magnitude and the range of orientational anisotropy and its dependence on the nature of the interface (non-polar, polar, or metallic) and the geometry of the interface (planar or curved).

1 Introduction

In recent years, computer simulation has matured into one of the most powerful theoretical techniques capable of investigating the complex structural, dynamic and chemical phenomena at the liquid/liquid or liquid/solid interface on the molecular level. An increasing number of reviews bears witness to this development [1–8]. The principal strength of the method is its ability to treat simple molecular models, which can also be investigated by more traditional theoretical techniques, and complex realistic models, which are fair representations of real world chemical systems, on an equal footing. Consequently, molecular dynamics (MD) and Monte Carlo (MC) simulations are at present the methods of choice for the theoretical investigation of realistic models of interfaces.

Most interfacial properties of real materials are the consequence of symmetry breaking and the ensuing anisotropy of molecular interactions within rather small characteristic distance ranges from the interface. Especially in polar media, static orientational correlations between different molecules, reorientation phenomena, and orientational correlations between molecules and the

¹ Author to whom correspondence should be addressed.
Electronic mail: eckhard.spohr@chemie.uni-ulm.de

interface are at the heart of this anisotropy. In the present paper we review our current understanding of orientational properties of water and aqueous electrolyte solutions in the vicinity of solid phases. The manuscript is based on a lecture one of us (ES) presented at the European Research Conference on “Orientational Order and Dynamics in Liquids and Glasses” in Crete, 1997. We illustrate the orientational properties using several examples taken from our own work on different interfacial systems:

- water at simple non-polar interfaces,
- water at metallic interfaces,
- aqueous electrolyte solutions at metallic interfaces, and
- water-filled cylindrical pores with and without chemical functionality.

Similar problems that are being actively investigated by a number of groups include

- the behavior of water near and inside biological membranes (e. g., [9–15]),
 - the hydration of large proteins (e. g., [16–18]),
 - the adsorption of water in slit pores and its relation to the “surface force” (e. g., [19–21]),
 - the structure of water in “vycor” and other glass pores (e. g., [22]),
 - adsorption in zeolites (e. g., [23]), and
 - the chemical dynamics at liquid-liquid interfaces (e. g., [24–30]),
- to name but a few.

In what follows we will first discuss some of the models used in computer simulations of realistic two-phase systems involving water and aqueous solutions and various aspects of orientational order in liquids near interfaces. We will then present a number of examples, followed by some general conclusions concerning the factors that govern the interfacial structure.

2 Models and Methods

The classical molecular dynamics (MD) simulation technique has been used in all simulations presented in this paper. This method is well established for the investigation of bulk water or aqueous electrolyte solutions. Consequently, the applied water model potentials are chosen from the multitude of models used in the simulation of bulk aqueous systems. These models are usually built by combining partial point charges in a rigid or flexible geometry with a short ranged repulsive potential. Examples for this class are the TIP4P [31], the SPC/E [32] or the BJH [33] models. Although none of these simple model potentials model *all* aspects of liquid water satisfactorily, they provide, to the very least, good qualitative insight and, if carefully chosen to the problem at hand, even quantitative results. One alternative, the *ab initio* Car-Parrinello (CP) molecular dynamics approach [34–37], is still computationally too costly for obtaining good statistics in bulk systems, let alone interfacial systems. The CP method has its stronghold in dealing with systems in which the chemical behavior changes with molecular geometry and where thus the *classical* methods fail (see, e.g., [38]), or in systems for which no adequate pairwise additive potentials have yet been developed. CP simulations have been performed for the adsorption of H₂O on MgO, surfaces where physisorption on smooth surfaces and dissociation on stepped surfaces were observed [39].

In simulations of electrolyte solutions, ions are usually described by charged spheres of a suitable diameter which interact through Coulomb forces with other ions and with the partial

charges of the water model and through short ranged potentials (often of the Lennard-Jones type). Models of this kind have been used successfully by many authors for a number of alkali, alkaline earth, and halide ions in aqueous solutions (see, e.g., [40–43] and references therein).

Non-polar surfaces are modeled by flat one-dimensional Lennard-Jones potentials [44–46], by an array of Lennard-Jones particles [45–47], which introduces a certain amount of surface corrugation into the model, or by the complete absence of interactions in the case of the free liquid/vapor interface [48–51]. Surfaces with polar functional groups are simplistically described by embedding point charges into a model of a non-polar surface or by explicit representation of the atomic surface structure with empirical molecular modeling force fields [22,45,52,53]. Metallic properties of surfaces are modeled either on the basis of the image charge model in combination with smooth or corrugated Lennard-Jones and Morse potentials [54–60], or through an array of metal atoms with metal-water potential functions derived from *ab initio* calculations [60–62]. While the latter approach can result in a more realistic simulation of the interface, the former model is, due to its heuristic nature, a simple means to investigate systematically the dependence of surface-induced effects in an electrochemical environment.

It has to be emphasized here, that the complexity of the system, which stems from the inhomogeneity and anisotropy near the interface, mandates the simulation of very long trajectories and/or very large systems in order to obtain statistically reliable results. Thus the reported simulations were performed for times between several hundreds of picoseconds and more than two nanoseconds. Consequently thermostatization had to be used in order to maintain a temperature of 298K in all simulations. The vast amount of computer resources needed for these simulations limits the extent to which systematic variation of model potentials is possible. Further details of the models will be discussed together with the results at the appropriate locations in the following sections. For more details on the simulation techniques and the models, the user is referred to the original publications and to standard texts like [23,63,64].

3 Orientational Correlations

In a homogeneous and isotropic medium the relative orientation between two rigid molecules is a complex function of six variables. A coordinate system can be defined by the principal molecular axis system of one molecule. The center of mass of the second molecule can be thought of as being located at the position (in spherical coordinates) (r, ϑ, ϕ) in the principal molecular axis system of the first one. The three Euler angles (α, β, γ) then specify the orientation of the second molecule relative to the principal axis system of the first one. Thus the orientational distribution can be completely described through a function $p(r, \vartheta, \phi, \alpha, \beta, \gamma)$. In practice, no experiments exist which are capable of extracting the full orientational distribution function. In principle, $p(r, \vartheta, \phi, \alpha, \beta, \gamma)$ can be calculated from a computer simulation, but there are also two practical limitations. One is the obvious problem of representability of a six-dimensional function and the other is the statistical noise in a distribution function where, even in very long simulations, only few configurations contribute to the average that forms the value p at a given point in six-dimensional space. Similar to analytical theory, one often resorts to an invariant expansion of the orientational distribution function in terms of Wigner matrices and spherical harmonics [65,66]. In bulk liquids, which contain not too many different atomic species, the liquid structure

is more often characterized by atom-atom or site-site correlation functions. These functions can be extracted from a series of neutron or X-ray diffraction experiments or calculated from computer simulations. The site-site correlation functions contain, however, less information about the orientational structure than the full distribution function, $p(r, \vartheta, \phi, \alpha, \beta, \gamma)$.

In the vicinity of an interface the complete description of orientational structure becomes even more complex. Anisotropy and inhomogeneity of space introduce three additional degrees of freedom each. They characterize the orientation of the principal axis frame of the first molecule relative to the external coordinate system and the translation of the principal axis frame relative to specific points at the interface. Clearly, the calculation of the resulting 12-dimensional distribution function is practically impossible. Furthermore, it would contain more information than can be readily digested. Thus, in simulations, but also in the analysis of experiments, the focus is often kept on single particle properties. Neglecting the role of the second molecule reduces the number of degrees of freedom to six. Integrating out (for the purpose of analysis only) the degrees of freedom associated with surface corrugation reduces this number to only three or four. Finally, in polar liquids like water, one is primarily interested in the properties of the molecular dipole and thus able to reduce the distribution function to one function, $p(z, \cos \vartheta)$, which contains only two essential degrees of freedom, the distance of the molecule from the surface, z , and the cosine of the angle ϑ between the molecular dipole direction, $\hat{\mu}$, and the surface normal, \hat{z} . Integrating over all possible dipole orientations leads to the so-called density profile, $\rho(z)$, which can also be regarded as the equivalent to the pair correlation function between a molecule and a ‘surface particle’. On the other hand, averaging $p(z, \cos \vartheta)$ over a certain distance range from the surface produces the orientational distribution, $p(\cos \vartheta)$, in this area.

In the following we will analyze $p(z, \cos \vartheta)$, the density profile, $\rho(z)$, and the orientational distribution, $p(\cos \vartheta)$, in some detail for several systems. The investigation of static and dynamic dipole-dipole correlation functions, which is related to the dielectric properties of the system and of collective dipole relaxation functions is beyond the scope of this work. Rather, we will concentrate on the correlations of water and ionic hydration shells with the external coordinate system imposed by the existence of the interface.

4 Results

4.1 Water near non-polar surfaces

One of the most simple systems to study by MD simulation is the interface between pure liquid water and a non-polar phase. Many simulation studies have shown that the orientational properties are very similar for water near its free surface and near a weakly interacting wall [44,48,51,67–79]. The strength of the interaction determines the range over which the interfacial structure differs from the structure of the bulk liquid. The recurring structural theme is the preferential alignment of molecular dipoles in directions parallel to the interfacial plane. Detailed analysis [44] has shown that this feature is due to the tendency to maximize the number of hydrogen bonds under the geometrical constraint of the interface. Various orientational distribution functions show traces of “ice-like” features. However, we note that the overall structure and dynamics of water near a non-polar interface, as obtained from simulations, is predominantly liquid-like.

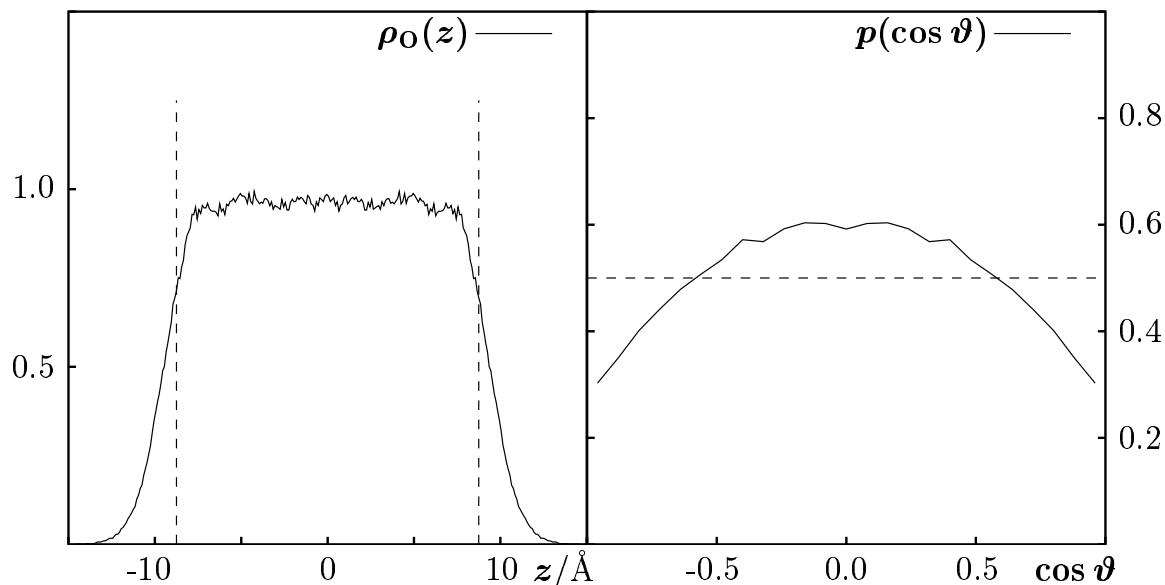


Fig. 1. Left: density profile, $\rho_O(z)$, from a 500 ps simulation of a thin film consisting of 200 TIP4P water molecules at room temperature [80]. Right: orientational distribution, $p(\cos \vartheta)$, with ϑ the angle between the molecular dipole moment direction, $\hat{\mu}$, and the surface normal, \hat{z} , for molecules in the range $|z| > 8.3 \text{ \AA}$ (indicated by the dashed vertical lines). The dashed horizontal line corresponds to an isotropic orientational distribution.

Figure 1 shows the oxygen density profile, $\rho_O(z)$, of a narrow slab of TIP4P water confined by two vapor phases (left) and the distribution of the cosine of the angle between molecular dipole moment and the outwardly directed surface normal, $p(\cos \vartheta)$, (right) for molecules in the surface layer ($|z| > 8.75 \text{ \AA}$) [80]. First, we note that the density distribution has a monotonic behavior near the interfaces; it does not exhibit large density oscillations. Second, the water/vapor interface at room temperature using this and other models is stable on the time scale of about 500 ps. The orientational distribution in the immediate vicinity of the interface shows a clear preference for configurations in which the molecular dipoles are aligned parallel to the surface plane. The observed alignment is driven by the tendency of the molecules in liquid water to maximize the number of hydrogen bonds. Water molecules being aligned almost parallel to the surface plane can participate easily in three hydrogen bonds, whereas molecules aligned perpendicularly to the surface plane are only able to form two hydrogen bonds with molecules in the liquid. Other possible arrangements with high hydrogen bond connectivity are less favorable, since they would give rise to a larger surface dipole with more repulsive long-range interactions within the interface.

4.2 Water near Metal Surfaces

The structure of water near polar and metallic surfaces — or, more generally, surfaces on which the water physisorption energy is reasonably large, i. e., in the range of 30-70 kJ/mol — is different from that near non-polar or free surfaces. Near metal surfaces, a distinct adsorbate layer interacts directly with the surface. Depending on the degree of ordering in this first layer,

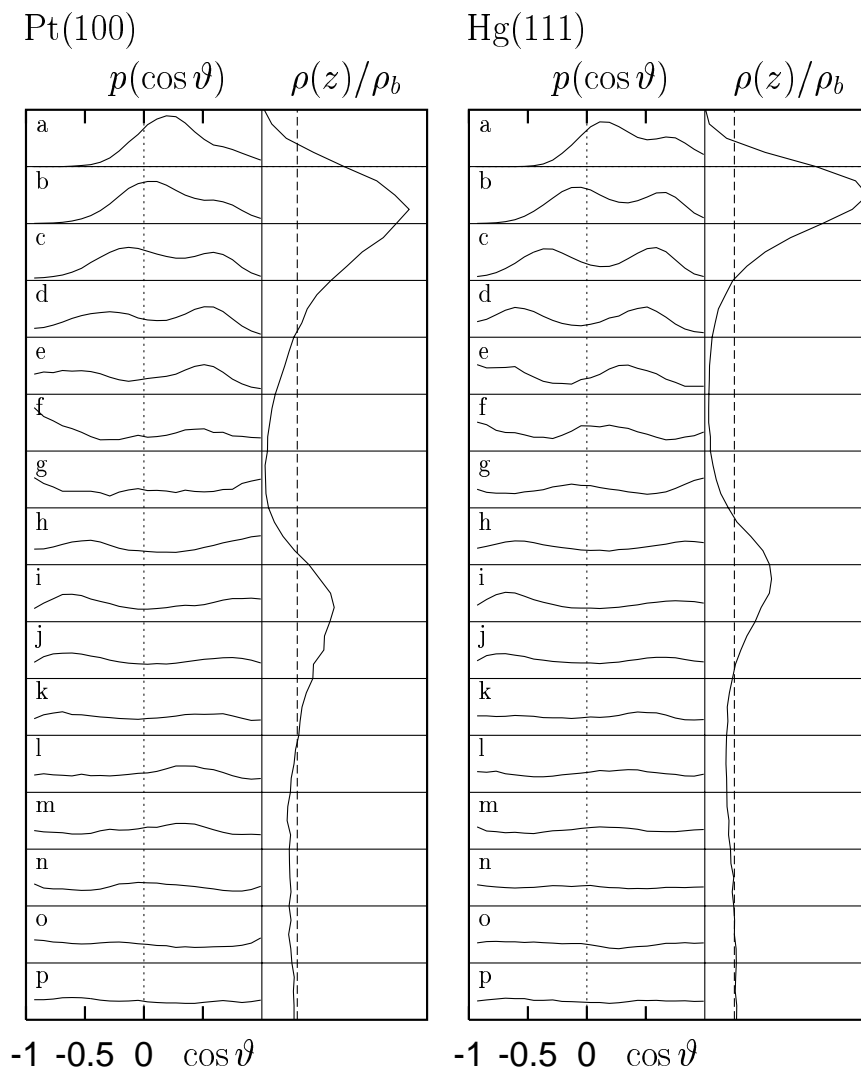


Fig. 2. Comparison of the orientational distribution of the water dipole moment on Pt(100) (left) and Hg(111) (right). $\cos \vartheta$ is the angle between the water dipole vector and the surface normal that points into the water phase. Panels *a* to *p* on the left are sampled from the distance intervals which are indicated by the cuts through the density profile $\rho(z)/\rho_b$ on the right.

an oscillatory density distribution develops. Its range depends on the details of metal, surface structure, and, in electrochemical experiments, applied potential. In most simulation studies, two to four distinct layers have been discerned, but for very high surface charge densities more pronounced ordering [81] or even a liquid/solid phase transition [82,83] has been observed. Similar layering is also seen in simple liquids near interacting interfaces (see, e. g., [84]).

The inhomogeneity (layering) near the water/metal interface is accompanied by orientational anisotropy. Again, one can rationalize some of the observed structural features in terms of maximization of hydrogen bonding. However, effects due to the specific nature of the interaction of water with the metal surfaces become important. Experimental evidence (see [85] and references therein) and quantum chemical calculations [86–95] have clearly shown that water

molecules interact with several metal surfaces through the oxygen atom, leading to a polarization of the interface.

The results of semi-empirical extended Hückel [86] and *ab initio* SCF cluster calculations [92] have been parameterized to yield a set of pairwise additive metal oxygen and metal hydrogen potential functions for the platinum (100) and the mercury (111) surface, respectively [62,96]. Figure 2 compares the polarization near the two surfaces. In addition to the orientational distribution, $p(\cos \vartheta)$, the oxygen density profile is plotted on the right side of each figure. The density profiles clearly show two pronounced layers. A weakly pronounced third layer (not visible in the graph) is also present. The baselines between distribution functions cut through the density profile. The distribution function in each panel on the left side is for the subset of molecules that are located in the distance range between these lines on the right side. The distributions are broad, indicating a strongly disordered liquid-like orientational structure. By and large, the orientational distributions are quite similar in both systems. Over the first peak in the density profiles (panels *a* to *d*) there are almost no molecules with the dipole moment perpendicular to the surface, contrary to the expectations of quantum chemical calculations, which predict almost exclusively configurations in the range $\cos \vartheta > 0.5$. Within the adsorbate layer, there is a transition from the preference for orientations in which the dipoles point more or less into the solution (*a* and *b*) to one where a substantial fraction of the dipoles point more or less towards the surface (*c* and *d*). This behavior is characteristic for the “bilayer” model that has been proposed for the interpretation of the structure of water monolayers adsorbed on metal surfaces under ultra-high vacuum conditions. In summary, the actual orientational structure is largely dominated by water-water interactions, which change the orientational distribution compared to that of isolated molecules (see also [96]). The orientational anisotropy ranges as far into the liquid phase as the density inhomogeneities do (roughly up to panel *m*), with increasingly less pronounced features. Slightly beyond the second maximum in the density profile the orientational distribution is isotropic, as it has to be the case for a bulk-like liquid.

4.3 Polarization in the Electric Double Layer

Real electrochemical systems are interesting, not because of the solvent but because a variety of species are present next to the electrode with position-dependent concentration and in position-dependent charge states (or chemical states). The most fundamental system to study is a simple electrolyte solution near a metallic surface. A multitude of studies [5,97–106] has investigated alkali and halide ions but also Fe^{2+} and Fe^{3+} next to several model metal surfaces. Most studies were concerned with the properties of a single ion. Only few studies to date have investigated the structure of the double layer at finite concentration [107–109]. In these studies, the simple image charge model of a metal surface, which disregards specific interactions between metal and an ion, has been employed. When, like in electrochemical simulations, a thin film of electrolyte, where the charges are embedded in a medium of dielectric permittivity equal to one, is in contact with a conducting metal electrode of infinite dielectric constant, the values of the image charges are just the negative values of the real charges and the total system of real charges and image charges is electroneutral. This makes it possible to simulate, in a realistic way, electrolyte solutions in contact with a charged electrode surface. Positive or negative surface charges can be balanced by an excess of anions or cations in the solution; in turn, the surface charge can be regarded as

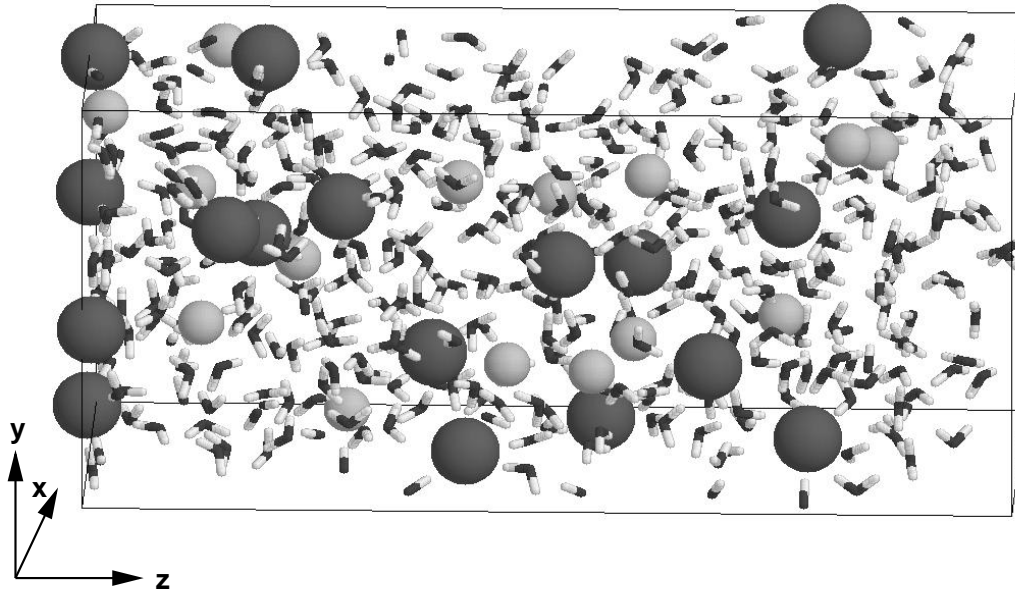


Fig. 3. Snapshot of a simulation of 15 Na^+ and 17 Cl^- ions dissolved in 400 SPC/E water molecules between a metal wall (left) and a free surface (right) [108,109]. Na^+ : small spheres, Cl^- : large spheres. The surface charge density of $\sigma = +9.9 \mu\text{C cm}^{-2}$ is the consequence of two excess image charges, which ensure total electroneutrality.

being produced by the images of the excess solution charges. For reasons of statistical efficiency, the concentration in these double layer studies has to be chosen rather high, in the range of 1 to 3 mol/l.

Figure 3 shows a snapshot of a 2.2 molal NaCl simulation from such a simulation. The metal surface is on the left. A rather well-defined first layer is discernible from the arrangement of ions and molecules near the left boundary. The aqueous film is confined on the right side by a vapor phase. It is stable on the simulation time scale of 2 nanoseconds, i.e., no molecules “evaporate”. Note that in this particular configuration there are 4 anions (large spheres) and one cation (small sphere) adsorbed on the metal surface so that the surface charge of $+2e$, e being the proton charge, is overscreened by the charges within the first layer.

From the density profiles of water molecules and ions (not shown here, see [108,109]) a pronounced second water layer can be inferred. The relatively strongly solvated Na^+ cations tend to be located between the first two water layers, building their (roughly octahedral) hydration shell from three molecules in each of the two layers. The preferred position of the chloride ions changes with surface charge. On positively charged surfaces, as in Fig. 3, some Cl^- anions are contact-adsorbed directly on the surface, while a negative surface charge pushes the equilibrium position away from the metal into the second layer of water molecules. In simulations of CsF solutions, the behavior of cations and anions is reversed. The preferred position of fluoride ions is in the second water layer, where they can form an almost unperturbed hydration shell. The fluoride position does not change significantly with the surface charge, contrary to the equilibrium position of Cs^+ , which is contact-adsorbed when the surface is negatively charged. In summary, the behavior can be interpreted as a competition between hydration and adsorption of

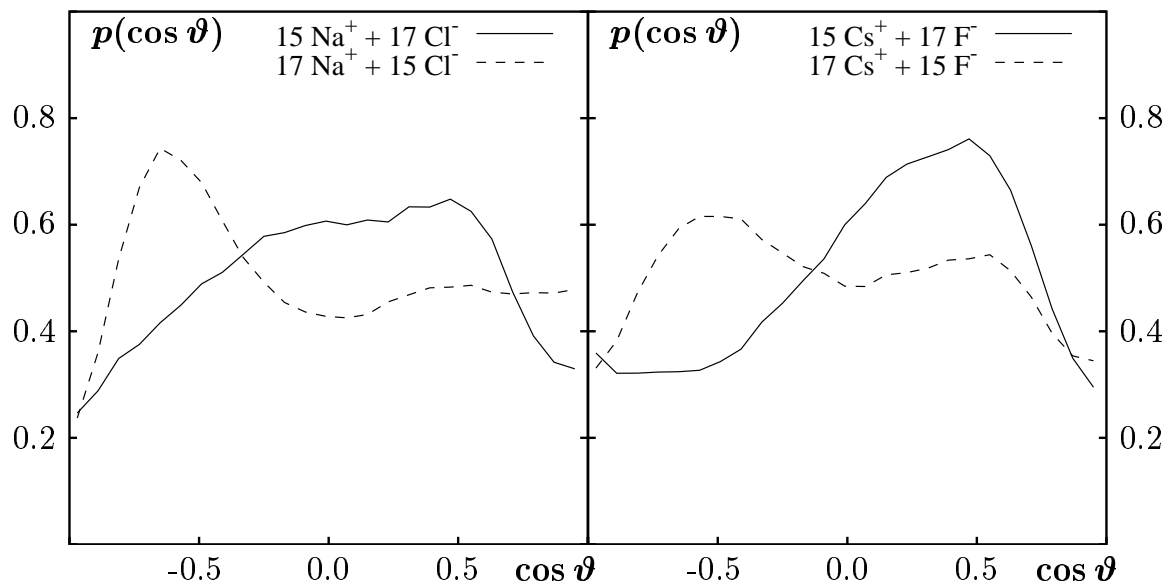


Fig. 4. Distribution the probability density of $\cos \vartheta$ in the first layer of molecules in simulations of 2.2 molal NaCl (left) and CsF solutions (right) at positive (full) and negative (dashed) surface charge densities (of magnitude $|\sigma| = 9.9 \mu\text{C cm}^{-2}$).

the ions. The large, weakly hydrated ions react more strongly to changes in the electric field of the electrode and are thus polarized to a larger extent.

The orientational distribution of water molecules in these concentrated solutions is different from that in pure interfacial water. Since the water dipoles contribute to the screening of the electrode charge, their orientation is dependent on it. The hydration of ions, however, also leads to well-known ordering effects and thus competes with the polarization due to the surface charge. Consequently, $p(\cos \vartheta)$ depends not only on the surface charge, but also on the charge and the equilibrium position of the ions close to the interface. Figure 4 shows $p(\cos \vartheta)$ for the four different cases of charged electrode surfaces studied by us. For both solutions there is a preference for values of $\cos \vartheta > 0$ (hydrogen atoms pointing away from the surface) at the positively charged electrode (full lines). Similarly, a preference for values of $\cos \vartheta < 0$ (hydrogen atoms pointing towards the surface) exists for negatively charged surfaces (dashed lines). This global behavior reflects the common reorientation property of dipoles upon change of the sign of an external electric field and is thus qualitatively of the same nature as the observed changes of the orientational distribution of pure water in an external electric field [82,83,110,111].

A comparison of the two different solutions at either the positive or the negative surface charge density reveals some characteristic differences. A positive surface charge imposes on water a force leading to orientations where the oxygen atoms are closer to the surface than the hydrogen atoms so that the average $\langle \cos \vartheta \rangle > 0$. In the CsF solution, this trend is enhanced relative to the NaCl case, since the interactions of water molecules with the F^- ions in the interlayer region between first and second layer also impose a force in the same direction. Consequently, the distribution becomes sharper, the maximum becomes higher and shifts towards slightly more

positive values in CsF than in NaCl solution. In the NaCl solution, water hydrates the contact-adsorbed Cl^- ions *within* the adsorbate layer and thus is more likely to have an orientation corresponding to values of $\cos \vartheta \leq 0$, as compared with the CsF solution.

Similarly, the orientational forces near the negatively charged surface due to the surface charge and due to the interlayer Na^+ ions are parallel and thus lead to an enhanced orientational ordering with a higher maximum around $\cos \vartheta \approx -0.65$ in NaCl solution than in CsF solution, where the orienting force due to the interlayer fluoride ions counteracts that of the surface charge. In summary, the orientational polarization of water is quite different in the two electrolyte solutions. It depends strongly on the nature of the electrolyte and its adsorption characteristics on the surface.

4.4 Water in Cylindrical Pores

Polymer membranes have become an important system component with a variety of interesting technological applications, e. g., for selective gas permeation, gas separation, or use in biosensors. Consequently, the characterization of structure and dynamics of synthetic pores on polymer basis or in inorganic materials has been a growing field of experimentation [112–122]. For a deeper understanding of the penetration of small molecules into these materials numerous theoretical studies were carried out (e. g., [123–129]).

Especially interesting are ion selective polymer membranes. Ion selectivity can be achieved by an appropriate choice of pore diameter and chemical modification with suitable polar functional groups. It is nowadays possible to synthesize polymer membranes with a chosen pore diameter in the range from a few to several hundred nanometers and a very narrow size distribution [130]. The transport properties of these membranes are expected to depend on the electric fields and thus orientational properties of the solvent within the pores.

We have recently started a project to study the transport properties of cylindrical model pores by MD simulation and relate them to structural elements inside the pore [46]. We first studied simple water-filled pores, confined by a cylindrical (10-4) Lennard-Jones potential, which interacts weakly (with average interaction smaller than thermal energy) with water molecules. These pores are non-polar in nature and serve as a reference against which to measure the properties of functionalized pores. We found that the center of pores with effective diameters of 1.5 nm and more exhibits a constant density region. With increasing pore size (we studied pores of up to 4 nm in diameter) this region grows and the calculated properties in the pore center (pair correlation function, orientational properties, hydrogen bond network, self diffusion coefficient, and orientational relaxation) slowly approach the corresponding values of the bulk liquid (TIP4P water, in this case). Near the non-polar pore surface, we find preferences for dipolar alignment parallel to the surface, similarly as in the case of the two-dimensional planar surfaces (see above) with small systematic, curvature-dependent differences. Water mobility in the non-polar pores is largest near the pore surface and approaches the bulk value from above towards the pore center.

We have then functionalized the model pores, for instance, by embedding 12 positive and 12 negative point charges into the surface of a cylindrical pore of length 67.9 Å in the following

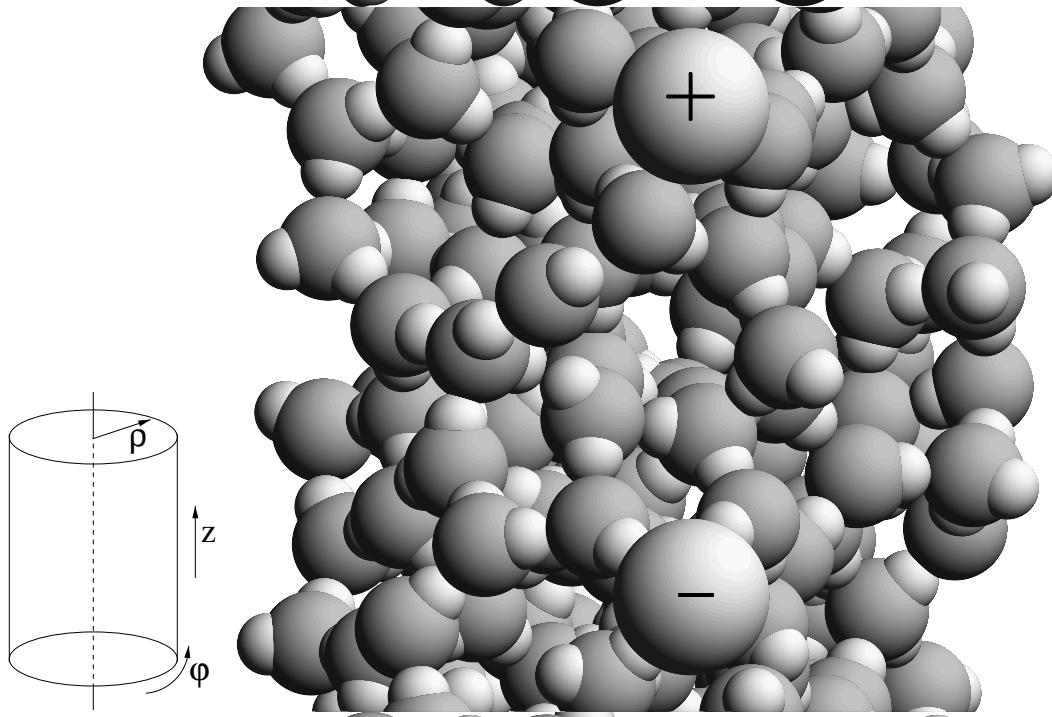


Fig. 5. Snapshot of a simulation of a cylindrical pore with SPC/E water molecules and surface charges (positioned alternately at $\rho = 11.1 \text{ \AA}$, the edge of the pore wall potential) [131]. The figure shows the region in the vicinity of two surface charges.

manner: Two charges with the same sign were put on the surface at the same value of z opposite to each other, the next two charges were put in a distance of $67.9\text{\AA}/12$ in z -direction, each shifted by $\Delta\varphi = 90^\circ$. The sum of the point charges equals zero. Figure 5 shows a portion of a configuration from such a simulation with effective pore diameter of about 1.8 nm. The surface charges are depicted as large spheres; note, however, that only the Coulomb interaction between the surface charge and water is of site-site type and that the repulsive part of the interaction stems from the presence of the otherwise smooth pore surface. One clearly recognizes the specific hydration of positive and negative surface charges; the degree of ordering in these hydration shells is similar to the one in bulk NaCl solutions.

Figure 6 shows the average molecular dipole moment along the ρ axis, μ_ρ , as a function of the distance ρ from the pore center (see Fig. 5 for definition). The average is normalized by the molecular dipole moment, μ . The central region is, in both cases, not polarized. In the non-polar pore (dashed line), molecules in an approximately 2 \AA wide region next to the surface enclose an average angle of about 100 degrees with the ρ axis ($\cos\vartheta \approx -0.2$). The hydrogen atoms point thus, on average, into the liquid, in order to maximize hydrogen bonding. Figure 7 supports this view. The orientational distribution function (dashed line) within the surface layer (defined here as $\rho > 6.0 \text{ \AA}$) shows the overall prevalence of parallel alignment. However, contrary to Figure 1, the distribution is more asymmetric reflecting the aforementioned orientational preference. This preference is due to packing constraints on the relatively strongly curved pore surface. If two neighboring molecules, located at the same values of z and ρ but different values of φ , form an

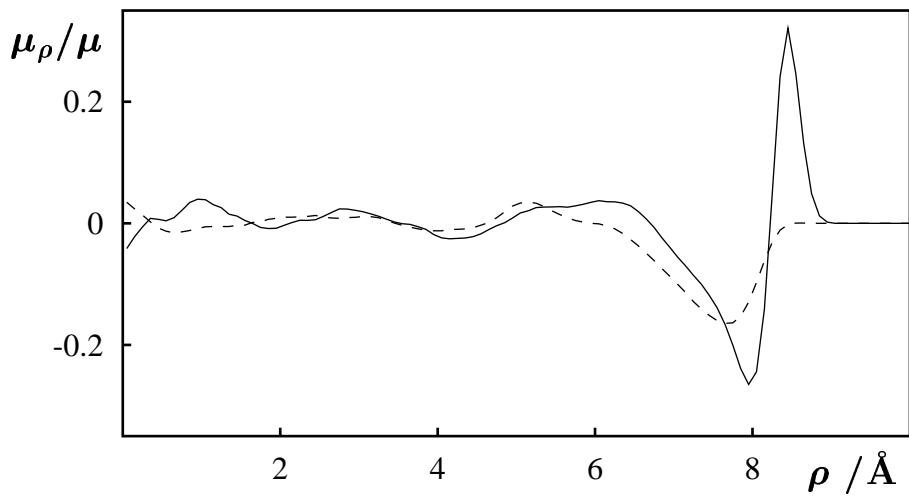


Fig. 6. Average dipole moment component, μ_ρ , along the radial direction, ρ , divided by the molecular dipole moment, μ , taken from two simulations using the TIP4P [31] water model. Full line: water in the functionalized pore (see text); dashed line: water in the non-polar reference pore.

ideal hydrogen bond, this will, at least for the molecule donating the hydrogen atom, result in a value of $\cos \vartheta = \hat{\mu} \cdot \hat{\rho} < 0$. The asymmetry of the orientational distribution becomes indeed smaller in larger pores (see [46]).

In the polar pore (full line), the average dipole moment along the radial direction has two regions of pronounced order close to the pore surface. Very close to the surface, molecules tend to be polarized with the hydrogen atoms toward the pore surface. Somewhat further away, molecules are polarized with the oxygen atoms towards the surface. A detailed analysis shows that this “double layer” formation has its origin in the hydration of the surface charges. This can be

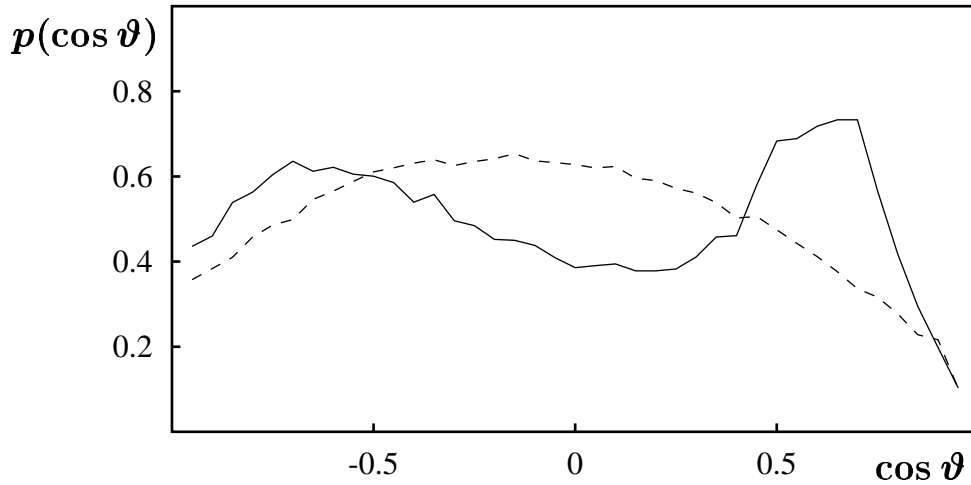


Fig. 7. Distribution of dipole orientations, $p(\cos \vartheta)$, relative to the ρ direction (see 5) close to the pore surface with radii larger than 6.0\AA . Full line: water in the functionalized pore surface (see text); dashed line: water in the non-polar reference pore.

inferred also from the snapshot in Fig. 5. Figure 7 clearly shows the bimodal distribution of molecular orientation in the range $\rho > 6.0 \text{ \AA}$. The maximum for $\cos \vartheta \approx -0.7$ is due to molecules hydrating positive surface charges, while the maximum $\cos \vartheta \approx +0.6$ shows the molecules hydrating negative surface charges.

Since in our pore model the hydrogen atoms do not interact with the repulsive core of the pore surface, they can approach the negative surface charges more closely than the oxygen atoms can approach the positive ones. Thus, the splitting of the radial distances at which the two dominant molecular configurations occur (in Fig. 6), is to a certain extent model dependent. However, the bimodal nature of the distribution function in Fig. 7 due to the hydration of different ions can be expected to be by and large independent of the details of the model.

The changes in orientational order near the pore surface lead to pronounced changes in water dynamics. While much of the transport in the non-polar pores occurs along the pore walls (the calculated diffusion coefficient is larger close to the surface), the formation of the more ordered double layer, which hydrates the surface charges, leads to an immobilization of water in the polar pore. Thus, water transport occurs primarily through the inner region of the pore. This, of course, has consequences on the mechanism of ion transport. Simulation studies in this direction are currently under way but have not been concluded yet.

4.5 Li^+ Adsorption on a Metal Surface

As a final example of how to analyze orientational correlations in interfacial computer simulations, we examine the adsorption of Li^+ on a mercury surface [5,106]. The conventional wisdom in electrochemistry based on interfacial capacitance measurements suggests that small ions like Li^+ should stay away from the electrode. Simulation studies, however found with several different models a tendency of small ions to move close to the electrode surface (see also the behavior of NaCl solutions discussed above). In the simulation discussed in the following, the interaction of water with the mercury surface is modeled by the *ab initio* potential of ref. [99]. The ion interacts with the surface through an image potential only. Thus, the study focuses on the role of water on the adsorption mechanism of a small alkali cation.

Figure 8 summarizes the key results of this study. The top frame shows the potential of mean force (PMF), $W(z)$, for the adsorption of the ion, normalized by the thermal energy. The PMF gives the Landau free energy of finding the ion at a position z in the simulation cell relative to its free energy in the bulk ($z \rightarrow -\infty$). The bottom frame contains the oxygen density profile monitored simultaneously in the same system. From the PMF curve it is clear that there exist two regions of minimal local free energy. The two regions are on the solution side of the first and second layer of water molecules, respectively (see bottom frame). The hydration number of Li^+ is slightly less than 6 in most regions. Around $z = -6.5 \text{ \AA}$ the hydration number is reduced significantly. This is the region in which the free energy rises while the ion crosses the second layer of water molecules. Once the ion is well within the second layer, it regains its full hydration shell. The rise in free energy is thus accompanied by a drop in hydration number. The ion maintains a more or less complete hydration shell up to very short distances from the surface ($z > -4 \text{ \AA}$), when it finally enters the water layer which is directly adsorbed on the

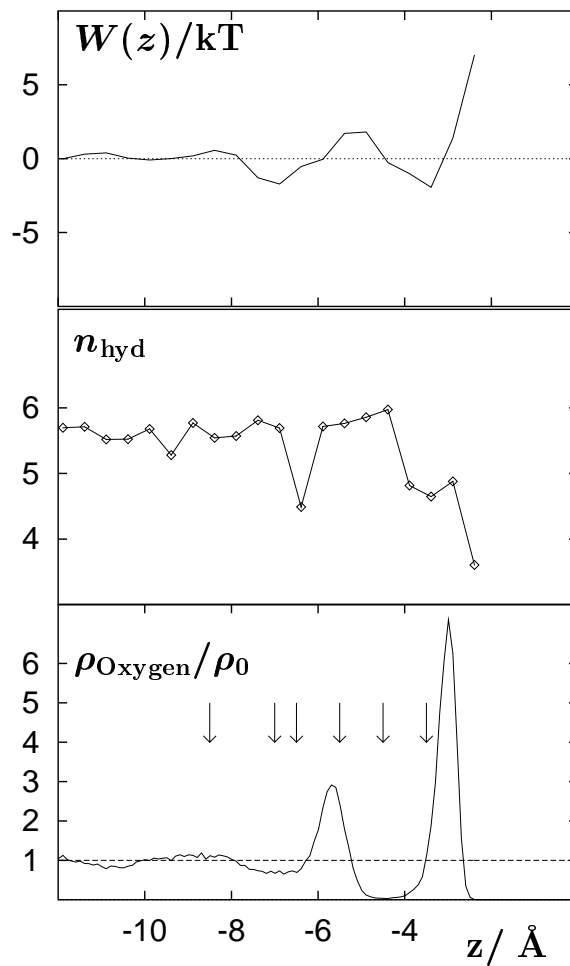


Fig. 8. Top: normalized potential of mean force, $W(z)/kT$, for the adsorption of Li^+ on the mercury surface; $T = 298.15\text{K}$ is the temperature and k is Boltzmann's constant. Center: The average hydration number of Li^+ , calculated as the running integral over the ion-oxygen radial distribution function up to its first minimum. Bottom: The oxygen density profile of water in the same system. The arrows indicate the positions at which the orientational distributions of the ion's hydration shell in Fig. 9 are evaluated. The coordinate scale is thus one where the metal surface is at $z = 0$ and the liquid phase is located in the negative half space.

surface, and the hydration number drops to values below 5.

In Fig. 9 the process is investigated in some more mechanistic detail. γ is the angle between a Li^+ -oxygen vector and the surface normal pointing towards the surface, as indicated in the inset. The figure shows, for six different positions of the ion (see arrows at the bottom of Fig. 8), the distribution of the cosine of this angle (full line) together with a running integral (dashed line), which is normalized such as to yield the hydration number of Fig. 8, when $\cos \gamma$ becomes one. Only water molecules in the first hydration shell of Li^+ are included. It is known from bulk simulations with similar models [132–134] that Li^+ forms a rather well-ordered octahedral coordination shell in bulk liquid water. At $z = -8.5 \text{ \AA}$ the distribution function exhibits 3 maxima. The running integration number shows that the two maxima at $\cos \gamma = \pm 1$ contribute one molecule each and that the broad maximum around $\cos \gamma = 0$ contributes four molecules

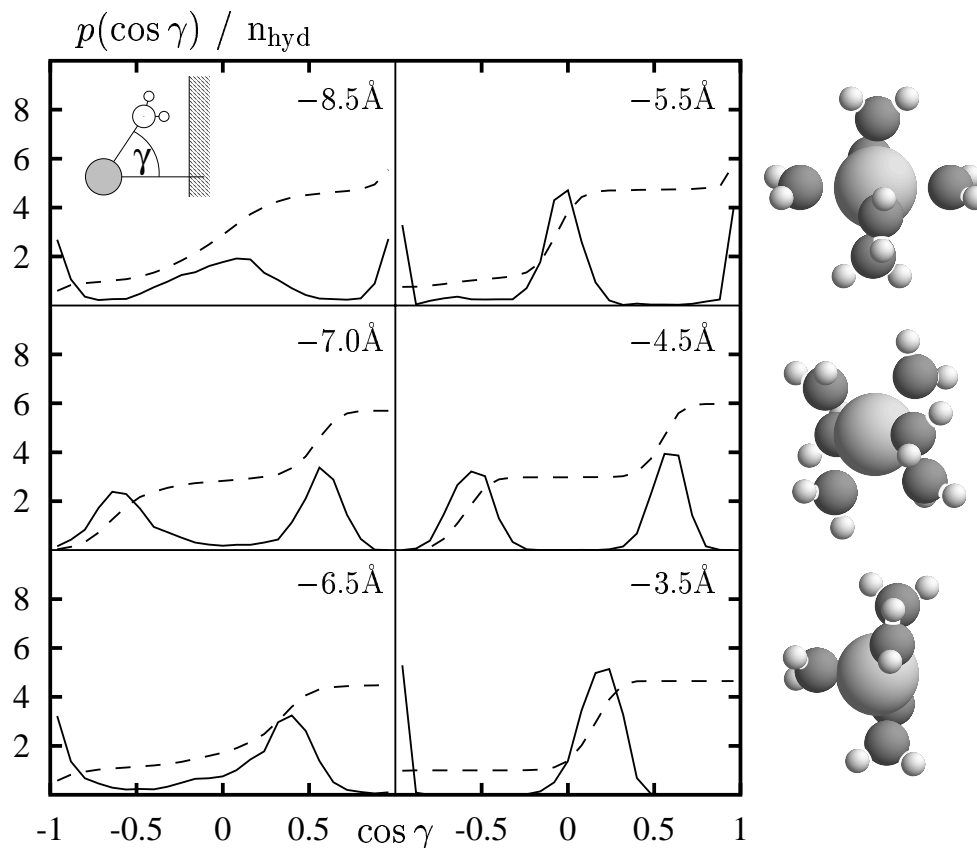


Fig. 9. Hydration shell distribution functions, $p(\cos \gamma)$, (full lines) at the various ion coordinates, z , indicated in the inset. γ is the angle between an ion-oxygen vector within the hydration shell and the surface normal pointing towards the metal surface (see drawing in upper left plot). The dashed lines indicate the running integral over the directions in which the hydration water molecules are found. The value at $\cos \gamma = 1$ is equal to the hydration number depicted in Fig. 8 at the appropriate position. The cartoons on the right sketch the structure and orientation of the hydration complex that is compatible with the corresponding distribution functions; with the metal surface (not shown) to the right of the hydration complex.

to the hydration shell. At this location, the octahedral $\text{Li}(\text{H}_2\text{O})_6^+$ complex points with one of its corners towards the surface, as indicated at the top right. Near the free energy minimum around $z = -7.0 \text{ \AA}$ the distribution function has only two maxima at $\cos \gamma \approx \pm 0.6$ which both contribute three molecules to the hydration complex. It is evident that this behavior corresponds to a rotation of the hydration complex so that the octahedron is now formed out of three water molecules in the second water layer and three molecules further in the bulk. In the corresponding distribution function for $z = -6.5 \text{ \AA}$ the hydration complex has rotated once more and consists now of only five water molecules in an approximately pyramidal configuration. The empty corner of an imaginary octahedron points towards the surface. The energetic expense to move one water molecule into the unfavorable region between the well-defined first and second water layers, where it can participate in the hydration complex, is obviously too high, so that the drop of the hydration number occurs.

At $z = -5.5 \text{ \AA}$, the octahedral complex is completed again, now formed out of one molecule in

the first water layer, four in the second layer and one further in the bulk. Before the ion reaches its second free energy minimum (the one corresponding to specific or contact adsorption) and loses again one water molecule from the hydration complex ($z = -3.5 \text{ \AA}$), the complex rotates once more ($z = -4.5 \text{ \AA}$); its structure and orientation is similar to that at $z = -7.0 \text{ \AA}$. In summary, the surprising observation that a small ion like Li^+ approaches the surface rather closely can be understood on the basis of the coupling between the translational motion towards the surface and a rotation of the hydration complex, which involves only at one instance a temporary reduction of the hydration complex in the style of an elimination-addition mechanism.

5 Summary

We have reviewed our current understanding of the nature and the extent of orientational order in liquid water and aqueous solutions near a variety of interfaces, mostly derived from the analysis of molecular dynamics simulation data. We have confined ourselves to the discussion of a few selected examples taken from the field of electrochemistry and material science, using realistic molecular models. We have mentioned related studies of interesting systems in biology, polymer science, inorganic chemistry and material sciences. The anisotropy and inhomogeneity in the interfacial region of these systems make an analysis of the data on the basis of, e. g., pair correlation functions like in the bulk difficult. Rather, we have focused on single-particle properties like atom density profiles and orientational distribution functions. To put these properties in perspective we have summarized some additional related results for which the reader is referred to the original communications.

We have demonstrated that the orientation of water molecules in the neighborhood of interfaces is the result of a competition between (i) the tendency to maximize the number of hydrogen bonds, (ii) the nature of the molecular forces governing adsorption, and (iii) the electrostatic requirement to minimize surface dipoles. Near non-polar surfaces, on which no adsorption occurs, or at the liquid/vapor interface, water molecules are predominantly aligned parallel to the interface; the orientational distribution is, however, broad. Near the metallic surfaces the strength of physisorption interactions becomes comparable in magnitude to the strength of hydrogen bonding interactions. Preferred orientations of adsorbed water molecules become more pronounced and show more clearly the signature of the metal surface, leading to the formation of distinct layers and to some lateral ordering induced by surface corrugation effects. By and large, the orientational order is still dominated by the requirements of the hydrogen bond network.

Orientalional order in electrolyte solutions near charged electrodes is determined by a complex interplay of several orienting forces. In addition to the physisorption and hydrogen bonding forces present in pure water near metal surfaces, ionic hydration induces order within, and even beyond, the first hydration shell, and the surface charge on an electrode polarizes water molecules in a characteristic distance interval determined by the Debye screening length. At the rather large ionic strengths in our simulations (2 mol/l), we observed that large, weakly hydrated ions like Cs^+ and Cl^- adsorb on negatively and positively charged metal surfaces, respectively, with partial loss of their hydration shell. This contact adsorption phenomenon weakens the orienting effect of the surface charge and reduces the orientational order. More strongly hydrated ions like Na^+ and F^- do not adsorb directly on the charged electrode but

in the region between the first and second adsorbed water layer. When the electrode carries a charge opposite to that of the ions, these ions enhance the orientational order of water near the metal surface, since the forces due to the surface charge and due to hydration point into the same direction.

In one case we have investigated the adsorption of a strongly solvated ion, Li^+ , in more detail. We find that the translation of the ion from the bulk to the surface is facilitated by a concurrent rotation of its octahedral hydration shell. The calculated small activation energy is due to a temporary elimination of only one water molecule from the ion's hydration shell when crossing the second water layer.

Orientalional order in cylindrical pores is governed by the same principles as order near planar surfaces. Non-polar pore surfaces lead to a similar alignment of dipoles parallel to the pore wall as for completely planar systems. Pores with embedded polar functional groups lead to the formation of a double layer. For the studied pores with typical diameter of a few nm, however, more molecules are affected by the pore surface than near planar interfaces. Consequently, properties of the liquid in these pores, like the diffusivity of molecules, are affected more strongly than near planar interfaces.

We conclude by stating that the ordering influence of the surface is rapidly dissipated in all the studied systems. The hydrogen bond network in liquid water is sufficiently flexible to adapt to different environments and recover its "native" structure within a few molecular diameters.

Acknowledgments

Financial support by the Fonds der Chemischen Industrie, the Clothilde Eberhardt Foundation and the European Science Foundation is gratefully acknowledged.

References

- [1] K. Heinzinger, in *Structure of Electrified Interfaces, Frontiers of Electrochemistry*, edited by J. Lipkowski and P. N. Ross (VCH, New York, 1993), Chap. 7. Molecular Dynamics of Water at Interfaces, p. 239.
- [2] M. L. Berkowitz and L. Perera, in *Theoretical and Computational Approaches to Interface Phenomena*, edited by H. L. Sella and J. T. Golab (Plenum Press, New York, 1994).
- [3] E. Spohr, Computer Modeling of Aqueous / Metallic Interfaces, Habilitationsschrift, Ulm, 1995.
- [4] I. Benjamin, Chem. Rev. **96**, 1449 (1996).
- [5] E. Spohr, G. Tóth, and K. Heinzinger, Electrochim. Acta **41**, 2131 (1996).
- [6] M. R. Philpott and J. N. Glosli, in *Solid-Liquid Electrochemical Interfaces*, Vol. 656 of ACS Symposium Series, edited by G. Jerkiewicz, M. P. Soriaga, K. Uosaki, and A. Wieckowski (ACS, Washington, 1997), Chap. 2. Molecular Dynamics Simulation of Interfacial Electrochemical Processes: Electric Double Layer Screening, pp. 13–30.
- [7] E. Spohr, in *Solid-Liquid Electrochemical Interfaces*, Vol. 656 of ACS Symposium Series, edited by G. Jerkiewicz, M. P. Soriaga, K. Uosaki, and A. Wieckowski (ACS, Washington, 1997),

- [8] P. A. Bopp, A. Kohlmeier, and E. Spohr, *Electrochim. Acta* (1997), in press.
- [9] M. L. Berkowitz and K. Raghavan, *Langmuir* **7**, 1042 (1991).
- [10] K. Raghavan, M. R. Reddy, and M. L. Berkowitz, *Langmuir* **8**, 233 (1992).
- [11] S.-J. Marrink, M. L. Berkowitz, and H. J. C. Berendsen, *Langmuir* **9**, 3122 (1993).
- [12] L. Perera, U. Essmann, and M. L. Berkowitz, *Langmuir* **12**, 2625 (1996).
- [13] S. J. Marrink and H. J. C. Berendsen, *J. Phys. Chem.* **100**, 16729 (1996).
- [14] M. Higa and A. Kira, *J. Phys. Chem.* **99**, 5089 (1995).
- [15] M. Higa, A. Tanioka, and A. Kira, *J. Phys. Chem. B* **101**, 2321 (1997).
- [16] V. Daggett, P. A. Kollman, and I. D. Kuntz, *Biopolym.* **31**, 285 (1991).
- [17] J. Guenot and P. A. Kollman, *J. Comp. Chem.* **14**, 295 (1993).
- [18] T. E. Cheatham, J. L. Miller, T. Fox, T. A. Darden, and P. A. Kollman, *J. Am. Chem. Soc.* **117**, 4193 (1995).
- [19] S. Murad, P. Ravi, and J. G. Powles, *J. Chem. Phys.* **98**, 9771 (1993).
- [20] D. E. Ulberg and K. E. Gubbins, *Mol. Simulation* **13**, 205 (1994).
- [21] E. Spohr, A. Trokhymchuk, and D. Henderson, *J. Electroanal. Chem.* , in press.
- [22] M. Rovere, private communication.
- [23] R. Haberlandt, S. Fritzsche, G. Peinel, and K. Heinzinger, *Molekulardynamik. Grundlagen und Anwendungen* (Vieweg, Braunschweig, Wiesbaden, 1995).
- [24] M. Hayoun, M. Meyer, and P. Turq, *Chem. Phys. Lett.* **147**, 203 (1988).
- [25] M. Meyer, M. Mareschal, and M. Hayoun, *J. Chem. Phys.* **89**, 1067 (1988).
- [26] M. Hayoun, M. Meyer, and P. Turq, *J. Phys. Chem.* **98**, 6626 (1994).
- [27] I. Benjamin, *J. Phys. Chem.* **95**, 6675 (1991).
- [28] I. Benjamin, *J. Chem. Phys.* **96**, 577 (1992).
- [29] I. Benjamin, *J. Chem. Phys.* **97**, 1432 (1992).
- [30] I. Benjamin, *Chem. Phys.* **180**, 287 (1994).
- [31] W. L. Jorgensen, J. Chandrasekhar, J. D. Madura, R. W. Impey, and M. L. Klein, *J. Chem. Phys.* **92**, 926 (1983).
- [32] H. J. C. Berendsen, J. R. Grigera, and T. P. Straatsma, *J. Phys. Chem.* **91**, 6269 (1987).
- [33] P. Bopp, G. Jancsó, and K. Heinzinger, *Chem. Phys. Lett.* **98**, 129 (1983).
- [34] K. Laasonen, M. Sprik, M. Parrinello, and R. Car, *J. Chem. Phys.* **99**, 9080 (1993).
- [35] M. Tuckerman, K. Laasonen, M. Sprik, and M. Parrinello, *J. Phys. Chem.* **99**, 5749 (1995).
- [36] M. Tuckerman, K. Laasonen, M. Sprik, and M. Parrinello, *J. Chem. Phys.* **103**, 150 (1995).
- [37] M. Sprik, J. Hutter, and M. Parrinello, *J. Chem. Phys.* **105**, 1142 (1996).
- [38] D. Marx, M. Sprik, and M. Parrinello, *Chem. Phys. Lett.* **273**, 360 (1997).
- [39] W. Langel and M. Parrinello, *Phys. Rev. Lett.* **73**, 504 (1994).
- [40] M. P. Tosi and F. G. Fumi, *J. Phys. Chem. Solids* **25**, 31 (1964).
- [41] K. Heinzinger, W. O. Riede, L. Schaefer, and G. I. Szasz, in *Computer Modeling Of Matter, ACS Symposium Series No. 86*, edited by P. Lykos (ACS, Washington, 1978), Chap. Molecular Dynamics Simulations Of Liquids With Ionic Interactions.
- [42] S. H. Lee and J. C. Rasaiah, *J. Phys. Chem.* **100**, 1420 (1996).
- [43] G. Tóth, *J. Chem. Phys.* **105**, 5518 (1996).
- [44] C. Y. Lee, J. A. McCammon, and P. J. Rossky, *J. Chem. Phys.* **80**, 4448 (1984).
- [45] S. H. Lee and P. J. Rossky, *J. Chem. Phys.* **100**, 3334 (1994).

- [46] C. Hartnig, W. Witschel, and E. Spohr, *J. Phys. Chem.* (1997), submitted.
- [47] B. Roux and M. Karplus, *Biophys. J.* **59**, 961 (1991).
- [48] M. A. Wilson, A. Pohorille, and L. R. Pratt, *J. Phys. Chem.* **91**, 4873 (1987).
- [49] M. A. Wilson, A. Pohorille, and L. R. Pratt, *J. Chem. Phys.* **99**, 3281 (1988).
- [50] M. Matsumoto and Y. Kataoka, *J. Chem. Phys.* **88**, 3232 (1988).
- [51] K. A. Motakabbir and M. L. Berkowitz, *Chem. Phys. Lett.* **176**, 61 (1991).
- [52] A. Delville, *J. Phys. Chem.* **97**, 9703 (1993).
- [53] A. Delville, *J. Phys. Chem.* **99**, 2033 (1995).
- [54] E. Spohr and K. Heinzinger, *Chem. Phys. Lett.* **123**, 218 (1986).
- [55] J. I. Siepmann and M. Sprik, *Surf. Sci. Lett.* **279**, L185 (1992).
- [56] J. I. Siepmann and M. Sprik, *J. Chem. Phys.* **102**, 511 (1995).
- [57] K. Foster, K. Raghavan, and M. Berkowitz, *Chem. Phys. Lett.* **162**, 32 (1989).
- [58] K. Raghavan, K. Foster, and M. Berkowitz, *Chem. Phys. Lett.* **177**, 426 (1991).
- [59] K. Raghavan, K. Foster, K. Motakabbir, and M. Berkowitz, *J. Chem. Phys.* **94**, 2110 (1991).
- [60] S.-B. Zhu and M. R. Philpott, *J. Chem. Phys.* **100**, 6961 (1994).
- [61] E. Spohr, *J. Phys. Chem.* **93**, 6171 (1989).
- [62] J. Böcker, R. R. Nazmutdinov, E. Spohr, and K. Heinzinger, *Surf. Sci.* **335**, 372 (1995).
- [63] M. Allen and D. Tildesley, *Computer Simulation of Liquids* (Clarendon Press, Oxford, 1987).
- [64] D. Frenkel and B. Smit, *Understanding molecular simulations: from algorithms to applications* (Academic Press, San Diego, 1996).
- [65] C. G. Gray and K. E. Gubbins, *Theory of molecular fluids. Volume 1: Fundamentals*, Vol. 9 of *The International series of monographs on chemistry* (Clarendon Press, Oxford, 1984).
- [66] W. A. Steele, *J. Chem. Phys.* **39**, 3197 (1963).
- [67] N. I. Christou, J. S. Whitehouse, D. Nicholson, and N. G. Parsonage, *Faraday Symp. Chem. Soc.* **16**, 139 (1981).
- [68] B. Joansson, *Chem. Phys. Lett.* **82**, 520 (1981).
- [69] R. Sonnenschein and K. Heinzinger, *Chem. Phys. Lett.* **102**, 550 (1983).
- [70] M. Marchesi, *Chem. Phys. Lett.* **97**, 224 (1983).
- [71] A. C. Belch and M. Berkowitz, *Chem. Phys. Lett.* **113**, 278 (1985).
- [72] N. I. Christou, J. S. Whitehouse, D. Nicholson, and N. G. Parsonage, *Mol. Phys.* **55**, 397 (1985).
- [73] R. M. Townsend, J. Gryko, and S. A. Rice, *J. Chem. Phys.* **82**, 4391 (1985).
- [74] G. Aloisi, R. Guidelli, R. A. Jackson, S. M. Clark, and P. Barnes, *J. Electroanal. Chem. Interfacial Electrochem.* **206**, 131 (1986).
- [75] J. P. Valleau and A. A. Gardner, *J. Chem. Phys.* **86**, 4162 (1987).
- [76] J. Hautman, J. W. Halley, and Y.-J. Rhee, *J. Chem. Phys.* **91**, 467 (1989).
- [77] A. Wallqvist, *Chem. Phys. Lett.* **165**, 437 (1990).
- [78] R. M. Townsend and S. A. Rice, *J. Chem. Phys.* **94**, 2207 (1991).
- [79] G. C. Lie, S. Grigoras, L. X. Dang, D.-Y. Yang, and A. D. Mclean, *J. Chem. Phys.* **99**, 3933 (1993).
- [80] E. Spohr, unpublished results.
- [81] M. Schlenkrich, K. Nicklas, J. Brickmann, and P. Bopp, *Ber. Bunsenges. Phys. Chem.* **94**, 133 (1990).
- [82] M. Watanabe, A. M. Brodsky, and W. P. Reinhardt, *J. Chem. Phys.* **95**, 4593 (1991).
- [83] X. Xia and M. L. Berkowitz, *Phys. Rev. Lett.* **74**, 3193 (1995).
- [84] D. Henderson, *Fundamentals of Inhomogeneous Fluids* (Marcel Dekker, New York, 1992).
- [85] P. A. Thiel and T. E. Madey, *Surf. Sci. Reports* **7**, 211 (1987).

- [86] S. Holloway and K. H. Bennemann, *Surf. Sci.* **101**, 327 (1980).
- [87] J. E. Müller and J. Harris, *Phys. Rev. Lett.* **53**, 2493 (1984).
- [88] M. W. Ribarsky, W. D. Luedtke, and U. Landman, *Phys. Rev. B* **32**, 1430 (1985).
- [89] H. Yang and J. L. Whitten, *Surf. Sci.* **223**, 131 (1989).
- [90] M. Rosi and C. W. Bauschlicher Jr, *J. Chem. Phys.* **90**, 7264 (1989).
- [91] H. Sellers and P. V. Sudhakar, *J. Chem. Phys.* **97**, 6644 (1992).
- [92] R. R. Nazmutdinov, M. Probst, and K. Heinzinger, *J. Electroanal. Chem.* **369**, 227 (1994).
- [93] S. Jin and J. D. Head, *Surf. Sci.* **318**, 204 (1994).
- [94] M. D. Calvin, J. D. Head, and S. Jin, *Surf. Sci.* **345**, 161 (1996).
- [95] A. Ignaczak and J. A. N. F. Gomez, *J. Electroanal. Chem.* **420**, 209 (1997).
- [96] E. Spohr and K. Heinzinger, *Ber. Bunsenges. Phys. Chem.* **92**, 1358 (1988).
- [97] J. Seitz-Beywl, M. Poxleitner, and K. Heinzinger, *Z. Naturforsch.* **46a**, 876 (1991).
- [98] D. A. Rose and I. Benjamin, *J. Chem. Phys.* **95**, 6956 (1991).
- [99] D. A. Rose and I. Benjamin, *J. Chem. Phys.* **98**, 2283 (1993).
- [100] J. N. Glosli and M. R. Philpott, *J. Chem. Phys.* **96**, 6962 (1992).
- [101] J. N. Glosli and M. R. Philpott, in *Microscopic Models of Electrode-Electrolyte Interfaces*, edited by J. W. Halley and L. Blum (Electrochemical Society Inc., Pennington, 1993), No. 93-5, pp. 90–103.
- [102] J. N. Glosli and M. R. Philpott, *J. Chem. Phys.* **98**, 9995 (1993).
- [103] E. Spohr, *Chem. Phys. Lett.* **207**, 214 (1993).
- [104] O. Pecina, W. Schmickler, and E. Spohr, *J. Electroanal. Chem.* **394**, 29 (1995).
- [105] E. Spohr, *J. Mol. Liquids* **64**, 91 (1995).
- [106] B. Eck and E. Spohr, *Electrochim. Acta* **42**, 2779 (1997).
- [107] M. R. Philpott and J. N. Glosli, *J. Electrochem. Soc.* **142**, L25 (1995).
- [108] E. Spohr, *J. Electroanal. Chem.* (1997), in press.
- [109] E. Spohr, *Electrochim. Acta* (1997), submitted.
- [110] G. Nagy and K. Heinzinger, *J. Electroanal. Chem.* **296**, 549 (1990).
- [111] A. M. Brodsky, M. Watanabe, and W. P. Reinhardt, *Electrochim. Acta* **36**, 1695 (1991).
- [112] J. H. Page, J. Liu, B. Abeles, H. W. Deckman, and D. A. Weitz, *Phys. Rev. Lett.* **71**, 1216 (1993).
- [113] B. Abeles, L. F. Chen, J. W. Johnson, and J. M. Drake, *Israel J. Chem.* **31**, 99 (1991).
- [114] A. B. Shelekhin, S. Pien, and Y. H. Ma, *J. Membr. Sci.* **103**, 39 (1995).
- [115] Y. Hirama, T. Takahashi, M. Hino, and T. Sato, *J. Colloid Interface Sci.* **184**, 349 (1996).
- [116] F. Katsaros, P. Makri, A. Mitropoulos, N. Kanellopoulos, U. Keiderling, and A. Wiedenmann, *Physica B* **234-236**, 402 (1997).
- [117] M. Agamalian, J. M. Drake, S. K. Sinha, and J. D. Axe, *Phys. Rev. E* **55**, 3021 (1997).
- [118] P. T. Callaghan, A. Coy, T. P. J. Halpin, D. MacGowan, K. J. Packer, and F. O. Zelaya, *J. Chem. Phys.* **97**, 651 (1992).
- [119] Y. Guo, K. H. Langley, and F. E. Karasz, *Phys. Rev. B* **50**, 3400 (1994).
- [120] J. Lyou and R. E. Norberg, *J. Kor. Phys. Soc.* **26**, 81 (1993).
- [121] J. B. W. Webber, J. C. Dore, H. Fischer, and L. Vuillard, *Chem. Phys. Lett.* **253**, 367 (1996).
- [122] M. A. Gardner, J. C. Dore, A. N. North, and D. Cazorlaamoros, *Carbon* **34**, 857 (1996).
- [123] J. L. Vallés and J. W. Halley, *J. Chem. Phys.* **92**, 694 (1990).
- [124] H. Takeuchi, *J. Chem. Phys.* **93**, 2062 (1990).
- [125] R. M. Sok, H. J. C. Berendsen, and W. F. van Gunsteren, *J. Chem. Phys.* **96**, 4699 (1992).
- [126] A. Gusev and U. W. Suter, *J. Chem. Phys.* **99**, 2228 (1993).

- [127] F. Müller-Plathe, *J. Chem. Phys.* **94**, 3192 (1991). See Ref. [13].
- [128] C. S. Chassapis, J. K. Petrou, J. H. Petropoulos, and D. N. Theodorou, *Macromolecules* **29**, 3615 (1996).
- [129] D. N. Theodorou, Transition-state theory investigations of small molecule diffusion in glassy polymers, Preprint, 1997.
- [130] H. Gankema, M. A. Hempenius, and M. Möller, *Rec. Trav. Chim. Pay-Bas* **113**, 241 (1994).
- [131] C. Hartnig, unpublished results.
- [132] K. Heinzinger, *Physica* **131 B**, 196 (1985).
- [133] K. Heinzinger, P. Bopp, and G. Jancsó, *Acta Chimica Hungarica* **121**, 27 (1986).
- [134] K. Heinzinger, in *Computer Modelling Of Fluids Polymers and Solids*, edited by C. R. A. Catlow et al. (Kluwer Academic Publishers, Dordrecht, 1990), Chap. Molecular Dynamics Simulations of Aqueous Systems, pp. 357–394.